# Effects of Cavities at the Nicotinamide Binding Site of Liver Alcohol Dehydrogenase on Structure, Dynamics and Catalysis

Atsushi Yahashiri,[†] Jon K. Rubach,[‡] and Bryce V. Plapp*

Department of Biochemistry, The University of Iowa, Iowa City, Iowa 52242-1109, United States

ABSTRACT: A role for protein dynamics in enzymatic catalysis of hydrogen transfer has received substantial scientific support, but the connections between protein structure and catalysis remain to be established. Valine residues 203 and 207 are at the binding site for the nicotinamide ring of the coenzyme in liver alcohol dehydrogenase and have been suggested to facilitate catalysis with "protein-promoting vibrations" (PPV). We find that the V207A substitution has small effects on steady-state kinetic constants and the rate of hydrogen transfer; the introduced cavity is empty and is tolerated with minimal effects on structure (determined at 1.2 Å for the complex with NAD+ and 2,3,4,5,6-pentafluorobenzyl alcohol). Thus, no evidence is found to support a role for Val-207 in the dynamics of catalysis. The protein structures and ligand geometries (including donor−acceptor distances) in the V203A enzyme complexed with NAD+ and 2,3,4,5,6-pentafluorobenzyl alcohol or 2,2,2-trifluoroethanol (determined at 1.1 Å) are very similar to those for the wild-type enzyme, except that the introduced cavity accommodates a new water molecule that contacts the nicotinamide ring. The structures of the V203A enzyme complexes suggest, in contrast to previous studies, that the diminished tunneling and decreased rate of hydride transfer (16-fold, relative to that of the wild-type enzyme) are not due to differences in ground-state ligand geometries. The V203A substitution may alter the PPV and the reorganization energy for hydrogen transfer, but the protein scaffold and equilibrium thermal motions within the Michaelis complex may be more significant for enzyme catalysis.
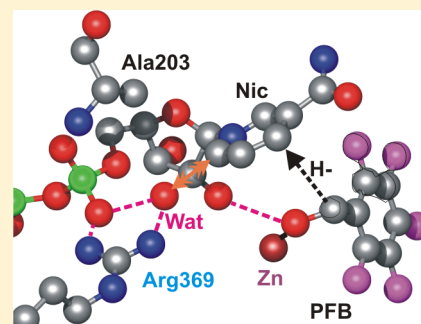
The contributions of protein dynamics to enzyme catalysis have been studied with great interest recently. Kinetic isotope effects provide evidence for quantum mechanical hydrogen tunneling for various enzymatic reactions, and the hydrogen transfer could be facilitated by protein motions that shorten the hydrogen donor−acceptor distance (DAD).[1−3] Fast protein motions could be coincidental, coupled, correlated, or in thermal equilibrium with the reaction coordinate.[4−10] The motions can involve the whole protein, as amino acid residues distant from the active site can act through connected networks.[11−13] Structural, kinetic, and computational studies of enzymes that are perturbed by site-directed amino acid substitutions can provide fundamental information about the roles of protein motions in catalysis.

Horse liver alcohol dehydrogenase (ADH, EC 1.1.1.1) is a good subject for these studies because structures can be determined at atomic resolution and the catalytic mechanism is well-described. X-ray crystallography of alcohol dehydrogenase has identified some of the dynamics involved in catalysis. The enzyme undergoes a global conformational change when coenzyme and substrate analogues bind.[14−16] X-ray crystallography also provides evidence for puckering of the reduced ring in ternary complexes with aldehyde analogues[17] and of the oxidized ring in complexes with fluoro alcohols.[18] Deformation of the nicotinamide ring may be important for the formation of the tunneling-ready state.[3,19−21] Horse liver ADH, as studied with its mutated forms, also exhibits kinetic isotope effects consistent with hydrogen tunneling.[22−25]

Schwartz and co-workers proposed that thermal motions, namely, "protein-promoting vibrations" (PPV), of specific amino acid residues facilitate the chemical reaction by modulating the distance between substrates, significantly affecting catalysis by lowering the height and shortening the width of the reaction barrier.[4,26−28] The calculations identified Ser-144, Gly-181, Val-203, Gly-204, Val-207, Glu-267, Ile-269, and Val-292 as residues in a conserved evolutionary sequence that contributes to PPV. The I269S substitution in the adenine binding site produced large increases in steady-state kinetic constants and made hydride transfer rate-limiting for ethanol oxidation, but with only a modest decrease in the rate constant for transfer.[16,29] The V292S substitution in the nicotinamide binding site also produced large increases in steady-state kinetic constants and made hydride transfer rate-limiting, but with only a 4-fold decrease in the rate constant for benzyl alcohol oxidation.[25]

The subjects of this study are Val-203, which contacts the nicotinamide ring, and Val-207, which is in a hydrophobic cluster near Val-203. Val-207 is highly conserved in dimeric ADHs, but the human class 1A and 1B isoenzymes and the plant enzymes have an alanine residue.[30] We expected that the V207A substitution should alter rate-promoting vibrations by creating a cavity and interrupting dynamic interactions. Large to small substitutions within the hydrophobic cores of enzymes

can lead to cavities, local shifts or collapse in structures, or introduction of water molecules.[31−33] A valine to alanine substitution can decrease protein stability by ∼2 kcal/mol, which should have a large effect on protein dynamics.[34,35]

Previous work showed that substitution of Val-203 (with Leu, Ala, or Gly) in ADH significantly decreases the catalytic efficiency for benzyl alcohol oxidation and diminishes the hydrogen tunneling, as compared to that of the reference F93W enzyme.[36] The V203A substitution moderately affects steady-state kinetic constants but decreases the rate of transfer of hydrogen from benzyl alcohol by 16-fold.[37] The diminished contribution of hydrogen tunneling was attributed to an apparent increase of 0.4−0.8 Å in the DAD for hydride transfer in the ground-state Michaelis complex, as compared to that of F93W ADH.[6,10,36,38] Molecular dynamics and normal-mode analysis suggest that anticorrelated motions of the catalytic and coenzyme binding domains can push the substrates together, and the V203A substitution could allow the nicotinamide ring to move away from the substrate and diminish the fraction of reactive conformations.[39−41] Theoretical analyses support the idea that the PPV would be modulated and the hydride transfer rate would be decreased in V203A ADH.[4,28,42] (Large to small substitutions of the homologous residue, Leu-176, in a thermophilic ADH also decreased catalytic turnover modestly and altered the temperature dependence of the kinetic isotope effect.[43]) However, the previous crystallographic studies were conducted on the NAD−2,2,2-trifluoroethanol (TFE) complexes of the F93W/V203A enzyme at 100 K at a resolution of 2.0 Å and of the V203A enzyme at 100 K and 2.5 Å, and those complexes were compared to the complex of the F93W enzyme determined at 277 K and a resolution of 2.0 Å as the reference structure. It is important to determine the structures in the same space groups and under the same conditions, and it would be relevant to determine structures of the complexes with a benzyl alcohol because it was used for the kinetics and isotope studies. In this work, atomic-resolution structures (1.1 Å) were determined for V203A ADH complexed with NAD$^+$ and 2,3,4,5,6-pentafluorobenzyl alcohol (PFB) or TFE, which are unreactive analogues of the good substrates, but not oxidized by the enzyme because of the strong electron withdrawing effects of the fluorines.

■ EXPERIMENTAL PROCEDURES

Materials. Reagent-grade chemicals were used as received unless specified otherwise. Alcohols and aldehydes were distilled prior to use. LiNAD$^+$ and Na$_2$NADH were obtained from Roche Molecular Biochemicals. Benzyl alcohol-α,α-d_2 (98.6% D) was obtained from MSD Isotopes. NADD [(4R)-[4-^{2}H]nicotinamide adenine dinucleotide] was prepared by reduction of NAD$^+$ with ethanol-d_5 by yeast ADH1 and purification by chromatography on DEAE-cellulose.[44]

Enzyme Preparations. The plasmid pBPP/EqADH1E, encoding the E isoenzyme found in the liver of domestic horse (*Equus caballus*, NCBI taxonomy ID 9796), GenBank accession number M64864, and UniProtKB entry P00327, was used for site-directed mutagenesis.[45] (The amino-terminal methionine residue is removed during protein processing *in vivo*, so that the sequence begins with Ser-1 and ends with Phe-374.) The Stratagene Quick Change method with degenerate oligonucleotide primers synthesized by Life Technologies was used to prepare the V207A and V207G substitutions. The forward primer had the following sequence (and the complementary reverse primer is implied), where the underlines and italics

mark the sites of mutation and an introduced *Fok*I recognition site, respectively: 5′-GGA GTG GGC CTG TCT (A/G)(T/C/G)T ATC ATG *GGA TGT* AAA GCA GCC-3′. Plasmids were transformed into XL1-Blue supercompetent cells, and transformants were selected on LB medium containing 100 μg/mL ampicillin and 12.5 μg/mL tetracycline. The V207A and V207G mutations were identified by digestion with the *Fok*I restriction enzyme and confirmed by sequencing of the complete coding sequence at The University of Iowa DNA Facility. The plasmid for the V203A enzyme was also prepared from the wild-type pBPP/EqADH plasmid and provided to us by J. P. Klinman.[36]

The recombinant wild-type, V203A, and V207A ADHs were expressed and purified according to the published procedure.[45] Purified enzymes showed a single band on polyacrylamide gel electrophoresis in the presence of sodium dodecyl sulfate with Coomassie blue staining and contained no bound nucleotides as the A_{280}/A_{260} ratio was 1.45. A standard enzyme assay was used for the calculation of specific activity,[46] and the protein concentration was determined with an extinction coefficient of 0.455 A_{280}/cm for a concentration of 1 mg/mL. The concentration of active sites was determined by titration with NAD$^+$ in the presence of pyrazole.[47]

Kinetic Studies. Solutions of coenzymes and substrates were prepared just before use. Concentrations of coenzymes and substrates were determined spectrophotometrically: ε_{260} = 18 mM^{-1} cm^{-1} for NAD$^+$, ε_{340} = 6.2 mM^{-1} cm^{-1} for NADH, ε_{256} = 200 M^{-1} cm^{-1} for benzyl alcohol, and ε_{248} = 12.5 mM^{-1} cm^{-1} for benzaldehyde. For all kinetics experiments, 33 mM sodium phosphate buffer with 0.25 mM EDTA (pH 8.0) at 25 °C was used. Initial velocity and inhibition studies monitored continuous NADH formation or oxidation on an SLM 4800C fluorimeter (λ_{ex} = 340 nm, and λ_{em} = 460 nm), with fitting of the progress curves to a line or a parabola to obtain the initial velocities. Inner filter effects at a high concentration (>10 μM) of NADH were corrected for. Cleland's programs SEQUEN and COMP[48] were used to calculate kinetic constants; errors on the estimates were <25% of the values.

Transient kinetics were studied with a BioLogic SFM3 stopped-flow instrument, with a dead time of 2.5 ms. The transient oxidation reaction was measured by following the change in absorbance at 332 nm after mixing 15 μN enzyme, 2 mM NAD$^+$, and varied concentrations (0.05−0.3 mM) of either protio benzyl alcohol or benzyl-α,α-d_2 alcohol.

X-ray Crystallography. Complexes of the mutated ADHs with NAD$^+$ and the fluoro alcohols were prepared as described previously.[18] The enzymes were first crystallized by dialysis of ∼10 mg/mL enzyme against 10% ethanol in 10 mM sodium phosphate buffer (pH 7.0) at 5 °C. The crystals were collected, redissolved in buffer with some added KCl, and dialyzed extensively at 5 °C against 50 mM ammonium *N*-[tris-(hydroxymethyl)methyl]-2-aminoethanesulfonate and 0.25 mM EDTA buffer (pH 6.7) (pH measured at 25 °C; pH 7.0 at 4 °C). Crystals suitable for X-ray were prepared by dialyzing ∼1 mL of 10 mg/mL enzyme against 10 mL of the pH 6.7 buffer and 1 mM NAD$^+$ and either 100 mM TFE or 10 mM PFB (K_i = 1.9 μM for V203A ADH[37]) at 4 °C by slowly increasing the concentration of 2-methyl-2,4-pentanediol to ∼13% by dialysis, when crystals formed. Then the concentration of diol was increased over several days to ∼25%, which provides cryoprotection at 100 K. The crystals were mounted on fiber loops and flash-vitrified by rapid immersion in liquid nitrogen for storage and data collection.

Data for a crystal of the complex of V203A ADH with NAD$^+$ and PFB were collected at 100 K using the synchrotron at the Advanced Photon Source at Argonne National Laboratories on June 16, 2007, on the GM/CA-CAT beamline with an X-ray wavelength of 1.0332 Å and a MAR300CCD detector, with high- and low-resolution passes (at a 120 mm crystal to detector distance with 0.25° oscillations, 360° total, and 1 s exposures, and at 193 mm with 0.5° oscillations, 360° total, with 0.5 s exposures). The data for a crystal of V203A ADH complexed with NAD$^+$ and TFE were collected on July 13, 2007, at the Advanced Light Source (ALS) in Berkeley, CA, using beamline 4.2.2, at 95 mm, an X-ray wavelength of 0.802 Å, 0.2° oscillations for 297 deg, with 6 s exposures. The data for the V207A ADH−NAD$^+$−PFB complex were collected on December 13, 2008, at ALS beamline 4.2.2 with an X-ray wavelength of 0.827 Å at 97 mm, with 0.25° oscillations over 360° total.

Data were also collected for the complex of V203A ADH with NAD$^+$ and PFB at ALS beamline 4.2.2 on December 12, 2012, on the new Research Detectors Inc. CMOS detector (282 mm × 295 mm) with shutter-less data collection at 100 mm at 1.25 Å wavelength, in an attempt to increase the magnitude of the anomalous signal for zinc. Oscillation frames were collected with a 0.1° rotation angle over 360° at a κ angle of 0° and over 180° at a κ angle of −20°. Data were processed with XDS[49] to give good data to 1.35 Å resolution.

Data for the reported structures were processed with d*TREK.[50] Structures were solved by molecular replacement with the coordinates for the refined structures of wild-type ADH complexed with NAD$^+$ and PFB or TFE [Protein Data Bank (PDB) entry 4DWV or 4DXH[18]]. The initial models used for refinement had alanine at the substituted sites and no fluoro alcohol, and the electron density maps showed no density for methyl groups for valine residues at position 203 or 207; however, there was clear density for the alcohols. The structures were refined by cycles of maximum likelihood, restrained refinement with REFMAC5[51] with riding hydrogens and anisotropic temperature factors in the final cycles. The monomer dictionary for NAD (named NAJ in our files) was modified to remove the restraints on planarity and to relax the restraints on bond distances for the nicotinamide ring so that puckered oxidized or reduced rings could be fit.[18] Model building used O.[52] The volume of the cavity created for V207A ADH was calculated by S. Ramaswamy with VOIDOO[53] using a probe radius of 1.0 Å and compared with that of the wild-type structure. Figures were prepared using the Molray web interface in Uppsala, Sweden.[54]

After refinement with REFMAC had been completed, SHELXL-2013[55] was used for 10 cycles of CGLS refinement and one full-matrix cycle of least-squares refinement (BLOC 1) with no restraints applied for the coenzyme, to calculate bond distances and angles and their errors for the nicotinamide ring and ligand interactions. Riding hydrogens were added to the protein, coenzyme, and fluoro alcohols. Errors were calculated with SHELXL-2013 using all unique reflections (MERG 2) and thus were slightly different from those calculated with SHELXL-97 previously.[18] Weighted averages for two subunits were calculated with EXCEL.

■ RESULTS

Preparation of ADHs. Mutagenesis with the degenerate oligonucleotide primers produced two different plasmids, encoding the V207G and V207A single substitutions in ADH,

and the active enzyme was expressed with both, as determined by the enzyme assay and staining for enzyme activity after electrophoresis on an agarose gel.[56] However, the V207G enzyme was not stable during purification, whereas the V207A enzyme could be purified to apparent homogeneity and thus could be studied further. Recombinant wild-type ADH was also purified for comparison. Titrations of active site concentrations of the soluble enzyme showed that ∼80% of the subunits of the V207A enzyme could bind NAD$^+$, whereas ∼60% of the V203A enzyme could; most preparations of the wild-type enzyme titrate at ∼80%. Turnover numbers based on the standard assay and active site titrations are listed in Table 1.

Table 1. Kinetic Constants for ADHs Acting on Benzyl Alcohol and Benzaldehyde[a]

kinetic constant	wild type[b]	V207A	V203A[c]
K_a (μM)	3.9 ± 1.0 (5)	5.0 ± 1.1 (5)	6.8
K_b (μM)	14 ± 1 (3)	13 ± 1 (8)	94
K_p (μM)	32 ± 8 (3)	62 ± 14 (4)	65
K_q (μM)	1.5 ± 0.6 (7)	3.2 ± 0.9 (7)	10
K_{ia} (μM)	20 ± 5 (5)	59 ± 5 (8)	29
K_{iq} (μM)	0.31 ± 0.02 (4)	0.39 ± 0.01 (4)	2.1
V_1/E_t (s^{-1})	3.0 ± 0.2 (6)	3.8 ± 0.7 (7)	2.2
V_2/E_t (s^{-1})	21 ± 1 (7)	38 ± 4 (4)	30
K_{eq} (pM)[d]	51	35	37
turnover number (s^{-1})[e]	1.6 ± 0.3 (1)	1.3 ± 0.2 (3)	4.6
k_{max}, oxidation (s^{-1})[f]	24[g]	30 ± 2	1.5
$^D k_{max}$, oxidation (s^{-1})[h]	3.6	2.7 ± 0.9	3.8

[a]Kinetic constants were determined at 25 °C in 33 mM sodium phosphate and 0.25 mM EDTA buffer (pH 8.0). K_a, K_b, K_p, and K_q are the Michaelis constants for NAD$^+$, benzyl alcohol, benzaldehyde, and NADH, respectively. K_{ia} and K_{iq} are the inhibition (dissociation) constants for NAD$^+$ and NADH, respectively. V_1/E_t is the turnover number for benzyl alcohol oxidation, and V_2/E_t is the turnover number for benzaldehyde reduction. Average values of the kinetic constants calculated from numerous trials (given in parentheses) in this study are given. [b]Recombinant ADH from this study. [c]The fits had errors of <25% of the values.[37] [d]K_{eq} is the Haldane relationship calculated from $(V_1 K_p K_{iq}[\mathrm{H}^+])/(V_2 K_b K_{ia})$. Values for the equilibrium constant have been reported to be between 35 and 70 pM.[100−102] [e]Turnover number determined in a standard enzyme assay with NAD$^+$ and ethanol at pH 9.0 and 25 °C, based on titration of active sites with NAD$^+$ in the presence of pyrazole. [f]Rate constant for transient oxidation of saturating concentrations of benzyl alcohol. [g]From ref 60. [h]The superscript signifies the H/D isotope effect for transient oxidation of protio benzyl alcohol as compared to the α,α-d_2 alcohol.

Kinetics of Wild-Type, V207A, and V203A ADHs. Steady-state kinetic constants were determined with initial velocity studies by varying the concentrations of both substrates (NAD$^+$ and alcohol or NADH and aldehyde) in a systematic manner (5 × 5 matrix of concentrations) and by product inhibition of one coenzyme against the other coenzyme as the varied substrate in order to determine the competitive inhibition (dissociation) constants for coenzymes. The kinetic constants for V207A ADH acting on ethanol and acetaldehyde were very similar to those found previously for the natural wild-type enzyme,[57,58] as were the kinetic constants with benzyl alcohol and benzaldehyde.[25,59] Because different experimental designs and experimenters can obtain kinetic constants that differ by 2-fold (or more), the experiments were repeated several times with recombinant wild-type and V207A enzymes, with the results listed in Table 1. In these experiments, the

initial velocity results in the direction of alcohol oxidation show the intersecting pattern typical of a sequential bi mechanism, but for aldehyde reduction, the patterns show parallel lines, which can arise if K_{iq} is smaller than K_q and the reduction is kinetically favored. Thus, the K_{iq} value was only determined by competitive inhibition of NADH against NAD+. The small standard deviations and the agreement of the K_{eq} value with experimentally determined values indicate that the kinetic constants are well-determined. The V207A substitution modestly (2−3-fold), but significantly, increased the values of K_p, K_q, and K_{ia}. The increased magnitude of K_{ia} with V207A ADH was also confirmed when the substrate was ethanol or acetaldehyde. For reference, Table 1 shows that the V203A substitution also increased several kinetic constants, but not K_{ia}.[37]

Transient kinetic studies of benzyl alcohol oxidation were used to study directly the hydride transfer step for these enzymes (Table 1). Wild-type ADH shows an exponential "burst" phase with a maximal rate constant of 24 s^{-1} at saturating alcohol concentrations (H/D isotope effect of 3.6) followed by a steady-state phase.[60] The two-phase reaction is characteristic of a rapid hydride transfer followed by slower release of NADH. Likewise, V207A ADH showed a burst phase with a maximal rate constant of 30 s^{-1}, and a substrate H/D isotope effect of 2.7, which was difficult to determine because the burst phase was not very distinct from the steady-state phase with the deutero benzyl alcohol. (The rate constant for the burst phase approximates the rate constant for hydride transfer, but simulations of the complete mechanism are required to obtain the microscopic value.[60]) In contrast, V203A ADH shows no burst phase, as hydride transfer is predominantly rate-limiting for turnover, with a rate constant of 1.5 s^{-1}.[37]

Isotope effects on steady-state kinetic parameters were determined by separate initial velocity studies with protio or deutero substrates (Table 2). The values for the wild-type and

Table 2. Isotope Effects for Steady-State Reactions of Benzyl Alcohol and Benzaldehyde Catalyzed by ADHs[a]

isotope effect	wild type[b]	V207A	V203A[c]
$^DV_1/E_t$	1.2 ± 0.1	1.7 ± 0.2	3.4 ± 0.2
$^DV_1/(E_tK_b)$	2.6 ± 0.8	2.7 ± 0.4	4.1 ± 0.6
$^DV_1/(E_tK_a)$	0.8 ± 0.2	1.1 ± 0.5	2.6 ± 0.7
$^DV_2/E_t$	1.2 ± 0.1	1.1 ± 0.1	1.1 ± 0.1
$^DV_2/(E_tK_p)$	2.6 ± 0.2	2.7 ± 0.4	3.1 ± 0.5
$^DV_2/(E_tK_q)$	1.0 ± 0.1	0.9 ± 0.1	0.75 ± 0.12

[a]Kinetic constants were determined at 25 °C in 33 mM sodium phosphate and 0.25 mM EDTA buffer (pH 8.0). The superscript D represents the ratio of kinetic constants with protio and deutero substrates. [b]Natural wild-type enzyme. [c]From ref 37.

V207A enzymes are similar. $^DV_1/E_t$ and $^DV_2/E_t$ values are somewhat larger than 1.0, $^DV_1/(E_tK_b)$ and $^DV_2/(E_tK_p)$ are more substantial, and $^DV_1/(E_tK_a)$ and $^DV_2/(E_tK_q)$ are 1.0 within errors. The results are consistent with an ordered bi-bi mechanism with coenzymes binding first and release of coenzymes being predominantly rate-limiting for catalytic turnover. In contrast, the mechanism of the V203A enzyme is partly random for oxidation of benzyl alcohol.[37]

X-ray Crystallography. Data collection and refinement statistics for the atomic-resolution structures are given in Table 3. The overall structures of the complexes with the V203A and

Table 3. X-ray Data and Refinement Statistics for Horse Liver ADHs Complexed with NAD+ and Fluoro Alcohols[a]

	V207A−PFB	V203A−PFB	V203A−TFE
PDB entry	4NFH	4NG5	4NFS
cell dimensions (Å)	44.5, 51.2, 92.3	44.5, 51.6, 92.6	44.3, 51.4, 92.5
cell angles (deg)	92.0, 103.0, 110.3	91.8, 103.1, 110.3	91.9, 103.1, 109.9
resolution range (Å)	20.0−1.2	17.9−1.1	19.6−1.1
no. of reflections (total, unique)	821122, 216747	1372121, 258723	810148, 263388
completeness (%) (outer shell)	94.2 (74.0)	86.2 (54.2)	88.3 (50.6)
R_{meas} (%) (outer shell)[b]	6.4 (42.9)	6.8 (29.7)	4.9 (47.4)
mean $\langle I \rangle / \sigma \langle I \rangle$ (outer shell)	11.3 (2.4)	15.5 (3.8)	12.2 (2.2)
R_{value}, R_{free}, test (%)[c]	13.5, 16.6, 0.5	12.0, 13.7, 1.0	13.8, 17.5, 1.0
rsmd for bond distances (Å)[d]	0.015	0.013	0.017
rmsd for bond angles (deg)[d]	1.89	1.79	1.93
estimated errors in coordinates (Å)	0.028	0.015	0.022
mean B value (Wilson, Refmac) (Å^2)	11.9, 17.0	10.5, 17.5	11.9, 17.9
total no. of atoms fitted	6939	7058	7024
atoms fitted, mean B value[e]			
protein (with alternative positions)	5767, 15.3	5828, 16.0	5826, 16.2
4 Zn, 2 NAD, 2 alcohols, 4 MRD[f]	150, 19.0	150, 19.5	136, 21.4
waters (with alternative positions)	1022, 32.6	1080, 32.2	1062, 34.9

[a]The space group is P_1 in all cases, with one dimeric molecule as the asymmetric unit. [b]$R_{meas} = R_{rim}$ (redundancy-independent merging).[50] [c]$R_{value} = (\sum |F_o - kF_c|)/\sum |F_o|$, where k is a scale factor. R_{free} was calculated with the indicated percentage of reflections not used in the refinement.[103] [d]Deviations from ideal geometry. [e]The data in the following three lines were calculated with the PARVATI server.[104] [f]MRD, (4R)-2-methylpentane-2,4-diol.

V207A enzyme are essentially identical to the corresponding structures of the wild-type enzyme, and they are in the "closed" conformation with NAD and the fluoro alcohols in an approximation of the Michaelis complex.[16,18] The electron density maps show well-defined positions for the NAD+ and the fluoro alcohols, which are very similar to those for the wild-type enzyme. In all of these complexes, the pro-R hydrogen of the alcohol is directed toward the re face of C4N of the nicotinamide ring, as would be expected for direct transfer of a hydride ion, as illustrated in Figures 2 and 4 in ref 18.

The electron density maps for the V207A enzyme clearly show that residue 207 is an alanine and that the local structures of V207A and wild-type ADHs are almost identical (Figure 1), and the structures (all α-carbons) superimpose with an overall rmsd of 0.10 Å. The high-resolution structures of ternary complexes of human ADH1A and ADH1B1 (with Ala-207) also superimpose well on human ADH1C2 (with Val-207) without significant conformational changes.[61] It is interesting that the bilobate cavity created by the V207A substitution does not affect the protein structure significantly, and no (less than 1/100 of the level observed for oxygens) electron density for new water molecules near Ala-207 is visible in the maps. The total volume available for waters in the cavity was calculated with VOIDOO to be 92 Å^3. There is no cavity near Val-207 in the wild-type ADH structure that can accommodate a water. Two water molecules could be positioned into the relatively
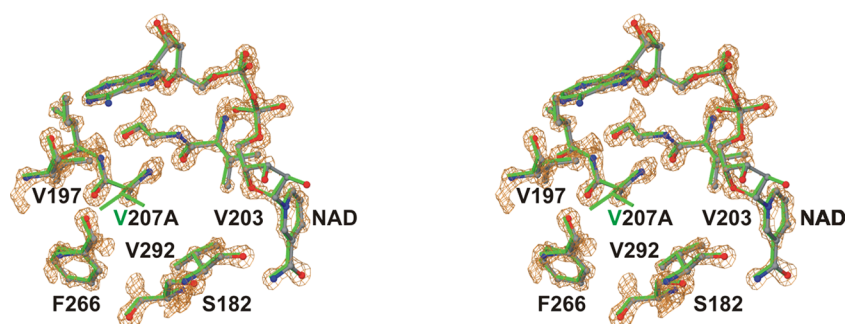
Figure 1. Structure and electron density of V207A ADH (PDB entry 4NFH) near residue 207. The space created by removal of two methyl groups is not filled. The structure of wild-type ADH in the same orientation is colored green (PDB entry 4DWV, 1.12 Å[18]).
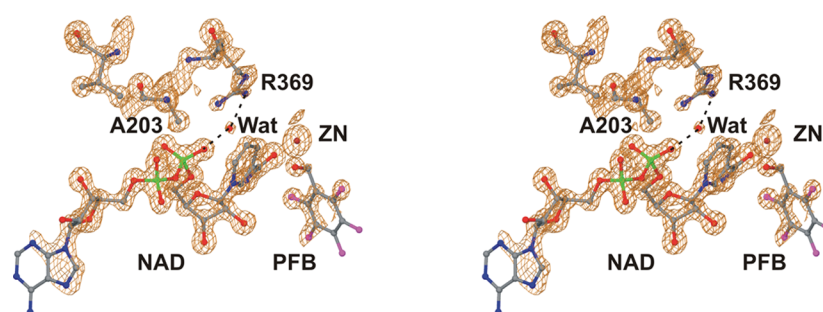

Figure 2. Structure and electron density of V203A ADH (PDB entry 4NG5) near residue 203. The space created by removal of two methyl groups is occupied by a water (red sphere) that contacts C6N of the nicotinamide ring of NAD and forms hydrogen bonds with the guanidino NH2 of Arg-369 and phosphate O1N atom of NAD. PFB with fluorines (magenta) and zinc (brown) are also shown.

apolar cavity in V207A ADH. One would be within van der Waals contact (3.2−3.5 Å) of aliphatic carbons of Gly-179, Ala-207, and valine residues 268 and 292. The other water could make a hydrogen bond with the O atom of Gly-179 but would make close contacts (3.0−3.1 Å) with side chains of Ser-183 (CB), Ala-207, and Phe-226. It is not likely that disordered water molecules are present in V207A ADH because the cavities are apolar (hydrophobic) and small (just large enough to accommodate waters) so that water should be detectable by X-ray crystallography, as concluded from a thoughtful review.[32] No waters were identified near Ala-207 in the human ADH1A and ADH1B1 structures.[61] Although cavities can destabilize protein structures, the protein scaffold of ADH is apparently able to maintain the structure when the bilobate cavity is empty of waters.

The electron density maps for the V203A complexes, with PFB or TFE, also clearly confirm the substitution at residue 203 (Figure 2). The structures of the wild-type and V203A ADH complexes are very similar. The wild-type (PDB entry 4DWV) and V203A ADHs complexed with PFB superimpose with an overall rmsd for all α-carbons of 0.13 Å. The wild-type (PDB entry 4DXH) and V203A enzymes complexed with TFE superimpose with an overall rmsd of 0.10 Å; the wild-type and the F93W/V203A (PDB entry 1A71[38]) enzymes superimpose with an rmsd of 0.18 Å. However, the major difference between the wild-type and V203A ADHs is that the cavity created by removing the two methyl groups introduces space for a new water molecule (labeled 994) that appears in both subunits A and B of the complexes with either PFB or TFE. This water molecule was identified, independently, in the F93W/V203A ADH structure.[38] This water makes a close contact to the nicotinamide ring of the NAD (3.1−3.2 Å to C6N) and forms good hydrogen bonds (2.8 Å) to the NH2 atom of the

guanidino group of Arg-369 and phosphate O1N atom of the NAD (Figure 2). In the wild-type enzyme, the CG2 methyl group of Val-203 is 4.5 Å from the NH1 atom of Arg-369 and 3.9 Å from the O1N atom of the phosphate of NAD; the V203A substitution creates a cavity in that space.

Artifactual Heterogeneity of Structure. It appears in the crystal structures that V203A ADH complexes have some heterogeneity because of the loss of some of the catalytic zinc, accompanied by a decreased occupancy of the fluoro alcohols and multiple conformations of some amino acids near the active site. Occupancies for catalytic zincs in both subunits of both complexes are estimated to be ∼60%, based on the electron density and comparisons of temperature factors with the structural zinc and with both zincs in the wild-type enzyme. The occupancy for the coenzyme does not appear to be affected, which is consistent with previous observations that the enzyme lacking the catalytic zincs still binds NAD^{+} and NADH, even though the enzyme is not catalytically active.[62] Crystallographic studies showed that NADH binds in about the same position, in the closed conformation of the zinc-free enzyme, as in the wild-type enzyme.[63] The occupancies of the fluoro alcohols are also decreased, to ∼75%, in the V203A enzymes. (These estimates are approximate, but the peak electron densities for carbons in the fluoro alcohols are ∼75% of those for the carbons in the imidazole group of His-67.) In the absence of the catalytic zinc, perhaps some fluoro alcohol binds weakly. The absence of the catalytic zinc also appears to allow an alternative conformation (∼20%) of Cys-46, where the sulfhydryl group of Cys-46 is rotated close to the carboxyl group of Glu-68. The rotation of Cys-46 in the zinc-depleted enzyme was observed before in crystal structures of the apoenzyme,[64] but not in the complex of the zinc-depleted
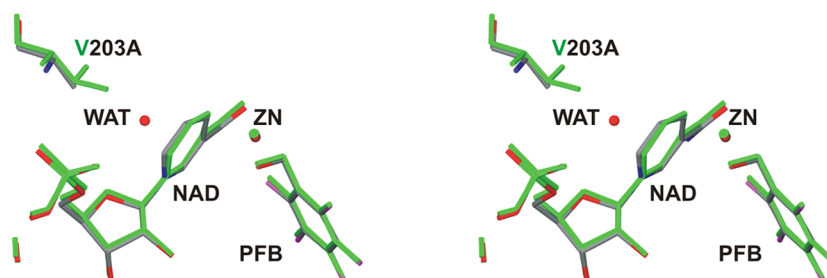
Figure 3. Comparison of structures of wild-type (green, PDB entry 4DWV) and V203A (atom coloring, PDB entry 4NG5) enzymes complexed with NAD and PFB shows a small difference in puckering of the nicotinamide ring. The water in the V203A enzyme is colored red and the zinc brown.

Table 4. Bond Distances and Geometry of Ligands in the Active Site

structure, PDB entry	average bond distances (Å) in the nicotinamide ring[a]					
	N1−C2	C2−C3	C3−C4	C4−C5	C5−C6	C6−N1
WT−PFB, 4DWV	1.345 ± 0.011	1.338 ± 0.013	1.445 ± 0.014	1.396 ± 0.015	1.356 ± 0.015	1.392 ± 0.012
WT−TFE, 4DXH	1.366 ± 0.012	1.379 ± 0.014	1.404 ± 0.014	1.366 ± 0.014	1.382 ± 0.015	1.380 ± 0.012
207A−PFB, 4NFH	1.373 ± 0.015	1.335 ± 0.019	1.431 ± 0.021	1.400 ± 0.021	1.368 ± 0.020	1.403 ± 0.017
203A−PFB, 4NG5	1.373 ± 0.011	1.362 ± 0.013	1.437 ± 0.015	1.443 ± 0.016	1.335 ± 0.015	1.405 ± 0.012
203A−TFE, 4NFS	1.334 ± 0.013	1.327 ± 0.015	1.476 ± 0.017	1.402 ± 0.019	1.358 ± 0.017	1.407 ± 0.015
	ligand distances (Å)			nicotinamide ring pucker		
	NAD C4N−ligand C[b]	Zn−ligand O1	O1−OG 48	α-C4 (deg)[c]	α-N1 (deg)[d]	twist (Å)[e]
WT−PFB	3.37 ± 0.02	1.96 ± 0.01	2.50 ± 0.01	5.6 ± 1.5	3.7 ± 1.5	0.038 ± 0.021
WT−TFE	3.44 ± 0.02	1.96 ± 0.01	2.45 ± 0.01	5.6 ± 1.6	3.9 ± 1.5	0.047 ± 0.020
207A−PFB	3.29 ± 0.02	2.00 ± 0.01	2.42 ± 0.02	4.9 ± 2.3	5.8 ± 2.1	0.056 ± 0.030
203A−PFB	3.40 ± 0.02	1.94 ± 0.01	2.52 ± 0.02	8.4 ± 1.4	8.0 ± 1.2	0.054 ± 0.018
203A−TFE	3.53 ± 0.03	2.00 ± 0.01	2.60 ± 0.02	12.6 ± 1.6	8.0 ± 1.7	0.037 ± 0.024

[a]Weighted average of the bond distances and errors for two subunits from refinement with SHELXL-2013 with no restraints on distances or planarity. [b]Ligand C is the "reactive" methylene carbon, C7 of benzyl alcohol and C1 (labeled C2 in the PDB entry) for TFE. [c]Angle between the C3−C4−C5 and C2−C3−C6 planes.[105] [d]Angle between the C2−N1−C6 and C2−C3−C6 planes. [e]Distortion of the boat conformation, defined as the distance between C5 and the C2−C3−C6 plane.

enzyme with bound NADH.[63] (The data for these structures are no longer available for closer inspection.)

It appears that the loss of catalytic zinc is associated with formation of alternative conformations in ~40% of the subunits of the V203A enzyme complexes. Arg-369, which usually interacts with the pyrophosphate of the coenzyme in the wild-type enzyme, has an alternative conformation that is retracted and instead interacts with the carboxyl group of an alternative conformation of Glu-68 and an additional, partially occupied water (labeled A or B 995). Slight changes in the positions of the side chains of Glu-68 and Arg-369 were also observed in the zinc-depleted enzyme.[64] Alternative conformations of Cys-170 and Leu-171 accommodate the changes in Glu-68. This network of alternative conformations (Arg-369, Glu-68, Cys-170, Leu-171, and a water) is not present in wild-type or V207A ADHs and does not appear to be an obligatory consequence of the V203A substitution because ~60% of the subunits have residue interactions that are similar to those for the wild-type enzyme. There is no steric imperative for the alternative conformations due to the V203A substitution. It appears that the set of alternative conformations may be an artifactual result of the loss of zinc due to handling of the protein sample, but these conformations could also be among the ensemble of structures that are available to the enzyme, as they could also be accommodated in the enzyme with the catalytic zinc. It should be noted that the previously determined structures of the V203A enzymes complexed with TFE (PDB entries 1AXG[36] and 1A71[38]) do not show any alternative

conformations, and the temperature factors are consistent with full occupancies for the catalytic zincs.

There are also some weak, unexplained densities (particularly in the active sites of V203A ADH complexed with TFE) where zinc ions associated with the phosphate O1N atom of the NAD, oxidized sulfur of Cys-46, or waters could be modeled at partial occupancies. However, anomalous difference electron density maps readily indicated the catalytic and structural zincs but showed no peaks that could be fit with a zinc at more than 0.05 occupancy as compared to the structural zincs. (The data collected at 1.0332 and 0.802 Å were used for these calculations, and the data at 1.25 Å were confirmatory.) Furthermore, refinement with partial occupancy of Cys-46 as a sulfenic acid gave unreasonable bond distances. Thus, our subsequent interpretations are based on the predominant structures, which represent ~60% of the molecules of the V203A enzyme complexes and ~100% of the V207A enzyme. Atomic-resolution structures offer the opportunity to see fine details of the structures, but interpretation of the electron density maps is challenging and remains incomplete. The assignment of occupancies is semiquantitative, as they are based on relative electron densities, and B factors for the alternative conformations may actually differ because of intrinsic motions of the atoms.

Geometry of Ligand Binding. The positions of the ligands (NAD and fluoro alcohols) in complexes of the V207A and V203A enzymes are very similar to the corresponding positions for the wild-type enzymes, but the position of the nicotinamide ring in the V203A ADHs differs slightly from that
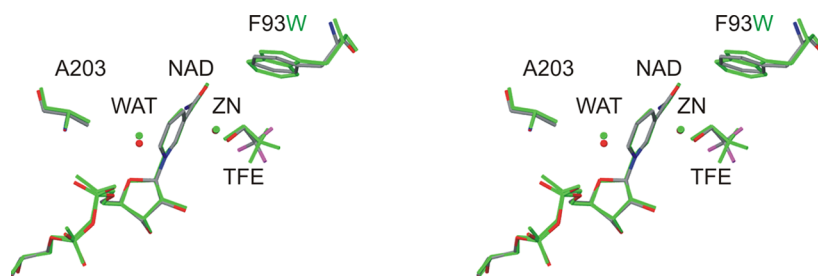
Figure 4. Comparison of structures of V203A enzymes complexed with NAD and TFE (PDB entry 4NFS, V203A, 1.12 Å, atom coloring; PDB entry 1A71, F93W/V203A, 2.0 Å, green) shows that the structures are remarkably similar. The aromatic rings of Phe-93 and Trp-93 and other atoms overlap, but the trifluoromethyl groups show a different rotation.

Table 5. Comparison of Active Site Distances of ADHs Complexed with NAD and Fluoro Alcohols[a]

structure, resolution, T	PDB entry	ligand	NAD C4N−ligand C	NAD C4N−203 CA	NAD C6N−203 CA
WT, 1.12	4DXH	TFE	3.44	5.50	4.52
V203A, 1.1	4NFS	TFE	3.53	5.47	4.20 (pucker)
F93W, 2.0, 4 °C	1AXE	TFE	3.16	5.65	4.48
V203A, 2.5	1AXG	TFE	3.83	5.40	4.22 (tilt)
F93W/V203A, 2.0	1A71	TFE	3.54	5.44	4.32 (tilt)
WT, 1.14	4DWV	PFB	3.37	5.41	4.51
WT, 2.1, 4 °C	1HLD	PFB	3.36	5.40	4.53
V207A, 1.2	4NFH	PFB	3.29	5.46	4.47
V203A, 1.1	4NG5	PFB	3.40	5.33	4.18 (pucker)

[a]The distances (Å) are averages of two subunits, in structures determined at 100 K unless noted otherwise.

in the wild-type enzyme (Figure 3). The atomic-resolution data and refinement with SHELXL permit a detailed analysis of the structures and geometry of binding (Table 4). The bond distances for the nicotinamide rings are well-estimated and are most consistent with a strained, oxidized ring with modest puckering, as described previously for the complexes of the wild-type enzyme.[18] The puckering angles for the nicotinamide rings in the complexes of V203A ADH are somewhat larger than those for wild-type ADH, but not as large as those observed for complexes of ADHs crystallized with NADH.[17,65,66]

However, the V203A enzymes appear to have ∼60% occupancy by the catalytic zinc, and the absence of the zinc in some active sites could allow the coenzyme to move or pucker more than for the wild-type and other mutated ADHs that retain the zinc. We tried to determine if the bound coenzyme was a mixture of NAD+ and NADH by refining the structures with alternative conformations (60:40 occupancies), but the bond distances were poorly defined, with errors of 0.2− 0.4 Å (as compared to 0.02 Å for one conformation). In addition, as shown in Table 4, the bond distances in the nicotinamide rings are not intermediate between oxidized and reduced nicotinamide rings. We conclude that the predominant structures for the active forms of the V203A enzyme contain NAD+, catalytic zinc, and the fluoro alcohol. The distances between C4N and the carbon of the alcohol from which hydrogen would be transferred are very similar among the respective complexes; however, the average distance in V207A ADH is 0.08 Å shorter than for wild-type enzyme, and the distances for the complexes with TFE are 0.09 Å longer in the V203A enzyme than in the wild-type enzyme. The catalytic zinc to alcohol oxygen distances are consistent with zinc alkoxide, and the distances between the alcohol oxygen and Ser-48 hydroxyl oxygen are consistent with a low-barrier hydrogen bond.

Comparison of Structures of ADHs Complexed with NAD and Fluoro Alcohols. The overall structures of the wild-type and mutated enzymes determined in this study are very similar to one another and to those previously determined for complexes of V203A, F93W, and F93W/V203A ADHs complexed with NAD and TFE. Indeed, the ligand positions in our V203A enzyme structure are essentially identical with those found in the F93W/V203A ADH complex previously described,[38] as shown in Figure 4. However, comparisons of the wild-type and V203A ADHs show some interesting and complicated small differences, as detailed in Table 5. The NAD C4N to "ligand C" distance is the putative distance for hydride transfer between the reacting carbons of the substrates in the ground-state model of the Michaelis complex. The value for the F93W enzyme (used as the "wild-type" reference, PDB entry 1AXE[36]) of 3.16 Å is clearly shorter than the value we found for the wild-type enzyme (3.44 Å, PDB entry 4DXH). This difference is not caused by the F93W substitution, as the indole rings superimpose on the benzene rings in these structures (rmsd of 0.24 Å for the coenzyme binding domains, residues 176−318, for PDB entries 4DXH and 1AXE). The F93W structure was determined at 4 °C, but the difference in temperature probably does not account for the shorter distance, as the wild-type structures with PFB (PDB entry 4DWV at 100 K and PDB entry 1HLD at 277 K) have similar C4N−ligand C distances, even though superimposition of the coenzyme binding domains (with an rmsd of 0.31 Å) shows that the molecule is slightly expanded at the higher temperature. Rather, it appears that the positions of TFE in the F93W (PDB entry 1AXE) and wild-type (PDB entry 1AXG) enzymes are somewhat different than in the wild-type enzyme determined at 1.12 Å (PDB entry 4DXH). It is most relevant that the NAD C4N−ligand C distances in the V203A enzymes (PDB entries 1A71 and 4NFS) are essentially identical and are ∼0.1 Å longer than the distance in the wild-type enzyme determined at 1.12 Å

(PDB entry 4DXH). The NAD C4N–ligand C distances in the complexes with PFB are also essentially the same (3.38 ± 0.02 Å), except that the distance in V207A enzyme is 0.08 Å shorter than for the wild-type enzyme.

It was previously proposed[38] that the increase in the C4N–ligand C distance due to the V203A substitution resulted from movement of the nicotinamide ring toward residue 203, because of removal of methyl group CG2 of Val-203, which is in van der Waals contact (3.64 Å) with NAD C6N.[18] The NAD C4N– or C6N–203 CA distances allow comparison of these enzymes and show the relative movement of the nicotinamide ring. The C4N–203 CA distances in the TFE and PFB complexes in the wild-type enzymes are very similar to the distances in the V203A enzymes, at an average of 5.43 Å (within 0.1 Å). (The distance is slightly longer for the F93W enzyme.) The NAD C6N–203 CA distances are very interesting because all of the V203A enzyme complexes have shorter distances (average of 4.23 Å) than for "wild-type" equivalents (average of 4.50 Å). This difference is due to a "tilt" of the nicotinamide rings in the structures determined previously, where crystallographic refinement restrained the planarity of the ring, or to ring puckering in this study, where no restraints on planarity were applied. The actual structures from the different studies may be similar even if the refinements produce different results.

Amplitudes of Motions from X-ray Crystallography. Although some enzymologists refer to protein structures determined by X-ray crystallography as "static" and possibly not the same as in solution, such structures provide, at least, average structures of thermodynamically accessible states, with dynamic aspects included in the temperature factors and defined alternative conformations (including "ensembles", which can be determined at atomic resolution). The structures can represent the best available view of the ground state for catalysis. For the structures of the V203A and V207A ADH complexes, the temperature factors and alternative conformations of residues at the active site are essentially the same as those for the wild-type enzyme. As noted before, leucine residues 57 and 309 have alternative conformations in the complexes of the wild-type enzyme with TFE or PFB, while the conformations of Leu-116 differ between the complexes with TFE and PFB due to interactions with the alcohols.[18] The V203A, V207A, and wild-type ADHs have essentially the same set of conformations. Although proteins are dynamic ensembles in global and local structure,[67] once the substrates are bound, as in the structures described here, it appears that hydrogen transfer would depend mostly upon the local dynamics. Using terms defined by others, we suggest that the complexes described here represent "preorganized"[6,10] states that approximate "tunneling-ready states"[21] of the substrates that form after modest "reorganization" involving fast protein and substrate motions.[12,68] We further suggest that the amplitudes of these motions can be estimated from dynamic information obtained from X-ray crystallography.

Temperature factors ("B", Debye–Waller, or anisotropic displacement, factors) provide information about fast motions in proteins but include contributions from the crystal lattice disorder, translations and rotations of pseudorigid subunits (TLS), internal collective motions, and local displacements.[69–73] A "residual" (or "local") temperature factor for particular residues can be calculated after removing the contribution of the "global" crystal lattice disorder and anisotropic motions of the subunits by TLS refinement in

REFMAC.[74] The local B factor would reflect fast motions and vibrations (nanosecond or faster), but not conformational changes (millisecond), which do not occur at 100 K.

Refinements (10 cycles of TLS followed by 10 cycles of maximum-likelihood restrained refinement of isotropic temperature factors) with the coenzyme binding and catalytic domains as TLS groups of the structures of wild-type and mutated enzymes studied here significantly decrease the B factors for individual atoms, but residual B factors are still large. The local B factors for residue 203 or residue 207 range from 5.5 to 8.6 Å^2, which would correspond to mean displacements of 0.26–0.33 Å, at 100 K [$\bar{u}_x = (B/8\pi^2)^{1/2}$]. The temperature dependence of the B factor increases by 4–5 Å^2 per 100 K,[75–77] so that at 300 K, the estimated local B factors could be ~16 Å^2, corresponding to mean displacements of 0.45 Å. Given such temperature factors, it appears that local equilibrium, vibrational, motions of the amino acid residues can be important factors in catalysis and would be comparable in the wild-type and mutated enzymes.

The equilibrium motions of the substrates could also decrease the DAD from 3.4 Å in the observed complexes to ~2.7 Å, where the hydride could transfer optimally. Refinements with the four domains of the two subunits and attached ligands as TLS groups (which decreased mean main chain B values from 16.0 to 9.0) produced average, residual B factors of 7 Å^2 for the atoms of the nicotinamide rings and 9 Å^2 for the carbons of the PFB for the wild-type enzyme. For V203A ADH, similar refinement with four TLS groups (which decreased mean main chain B values from 16.0 to 10.4) produced values of 10 and 12 Å^2 for the nicotinamide ring and the PFB, respectively. The nicotinamide ring has more interactions with the enzyme than does the benzyl alcohol, which is located in a hydrophobic pocket that accommodates a variety of alcohols. Thus, movement of the nicotinamide ring is somewhat restricted, whereas the benzyl alcohol could occupy an ensemble of states. Extrapolation to 300 K would give B values of 16–21 or mean displacements of up to ~0.5 Å. (The abstract graphic shows atoms with radii of 0.5 Å.) If the motions of the substrates are anticorrelated, it appears that the donor–acceptor distance could often approach 2.7 Å. This analysis of B factors is an approximation, because the B factors may be overestimated due to various contributions (errors in data and modeling, radiation damage, etc.) that are not accounted for, and the extrapolation from 100 to 300 K may be complicated by a "glass transition" at ~150 K.[75,78] [Analysis of the total, not "local", B factors for the structure of the wild-type enzyme complexed with NAD and PFB determined at 4 °C (PDB entry 1HLD) also indicates amplitudes of motion of 0.4–0.5 Å.] Nevertheless, it is significant that molecular dynamics simulations provide fluctuations of similar magnitude in ADH.[39,79]

■ DISCUSSION

The rationale for these experiments was that substitutions of valine residues near the nicotinamide binding site with alanine residues would produce cavities that would alter the local energetics, stability, interactions, and protein motions. Many studies suggest that protein dynamics are important for enzyme catalysis, but more direct experimental evidence is needed. In particular, structural studies are required to determine actual changes that might affect catalysis. This and previous studies show that cavity formation is accompanied by disparate effects on local structures and kinetics even though overall protein

structures and ligand binding are very similar. The results from this study do not provide support for a substantial contribution of PPV to catalysis, but they do raise questions about the roles of protein dynamics in catalysis and provide foundations for further computational studies that could relate structures to rates of catalysis.

V207A ADH. The V207A substitution caused only small changes in catalysis by ADH since both steady-state and transient-state kinetics were similar to those of the wild-type enzyme. Some 2−3-fold effects on steady-state constants are probably real, but catalysis is not altered substantially. The exponential burst phase for benzyl alcohol oxidation, reflecting hydride transfer, and isotope effects are essentially unchanged by the V207A substitution. The three-dimensional structure of the complex with NAD and PFB is also essentially unchanged, but the putative, "ground-state" hydride transfer distance is decreased by 0.08 Å compared to that of the wild-type complex. The cavity created by the substitution is apparently empty and not occupied by water molecules, and local crystallographic B factors are not affected, suggesting that the protein scaffold is quite stable and tolerates a cavity. We expected that the V207A substitution would affect the dynamics of the proposed PPV network. Because the structure of the complex and the rate of hydride transfer are essentially unchanged, the results provide no evidence that Val-207 participates in promoting vibrations. However, the results do not eliminate the possibility of such a contribution because many residues may cooperate in the vibrations and the quantitative effect on catalysis of the substitution of a side chain is not known. A "rough calculation" suggested that the promoting vibration in ADH lowered the free energy barrier by 30%, but further calculations are required.[80]

V203A ADH. The V203A substitution moderately alters the kinetics of ADH. The affinity for NADH and the catalytic efficiency for benzyl alcohol oxidation are decreased ∼4-fold, and the rate constant for hydride transfer for alcohol oxidation is decreased 16-fold, making hydride transfer a major rate-limiting step, as evidenced by a 3.4-fold deuterium isotope effect on the steady-state turnover.[37] Crystallography shows that the structures of the complexes of V203A and wild-type enzymes with NAD and TFE or PFB are very similar. The putative DAD (NAD C4N to methylene carbon of the alcohol) in V203A ADH complexed with TFE is increased by 0.1 Å relative to that in the wild-type ADH complex, but the distances are the same for wild-type and V203A ADHs for the complexes with PFB. The position of the nicotinamide ring is altered slightly in the complexes of V203A ADH with either TFE or PFB because of puckering that brings NAD C6N 0.3 Å closer to 203 CA than in the wild-type enzyme. The carboxamido N7N of the nicotinamide ring retains hydrogen bonds to the carbonyl oxygens of Val-292 and Ala-317 in the V203A enzyme, and the nicotinamide O7N retains the hydrogen bond to the backbone N of Phe-319. Interestingly, the removal of the CG2 methyl group of Val-203 has allowed a water molecule to bind, which is 3.1 Å from NAD C6N. The decreased affinity for NADH may be due to insertion of the water molecule and less favorable hydrophobic interactions near the nicotinamide ring.

Our kinetic and structural results differ from some previous results. The catalytic efficiency for benzyl alcohol oxidation was reported to have decreased by 36−44-fold with the V203A substitution relative to that of the wild-type or F93W enzymes,[36] whereas we found a 4-fold decrease.[37] This may be because the assay conditions are very different, but in any case, the decreased rate constant for hydride transfer and the altered isotope effects indicate that catalysis by the V203A enzyme has been compromised. The previous structural studies found an increase of 0.4−0.8 Å in the putative DAD, attributed to tilting of the nicotinamide ring toward residue 203.[36,38] The differences in the studies are not easily explained, but the atomic-resolution data presented here show that the structure and geometry of ligand binding of the V203A enzyme complexed with TFE (PDB entry 4NFS) are almost identical with those of the F93W/V203A enzyme complexed with TFE (PDB entry 1A71). In contrast, the geometry of the ligands in the "wild-type" reference enzymes (PDB entries 4DXH and 1AXE) is different, mostly because of the positioning of the TFE.

Because the V203A substitution has only small effects on the structures of the enzyme complexes, whereas the kinetics are affected, it appears that the results are consistent with the proposal that Val-203 participates in PPV. However, it remains to be determined if and how protein motions are coupled to the reaction coordinate and account quantitatively for the 16-fold effect on hydride transfer by the V203A substitution.[80,81] Furthermore, the insertion of the water near the nicotinamide ring in V203A ADH could affect the chemistry of hydride transfer because the water interacts closely with the negatively charged phosphate O1N and positively charged Arg-369 NH2, which should affect the electrostatics near the nicotinamide ring. In Val-203 ADH, a methyl group may act as an insulator between the charged groups and the nicotinamide ring. The roles of nearby oxygens appear to be a general issue, because a comprehensive survey of 340 PDB entries for enzymes with bound NAD(P) showed that 75 structures had 153 close contacts (<3.2 Å) between the nicotinamide ring and oxygen atoms of water or protein residues; several structures also showed puckered nicotinamide rings.[66] Quantum mechanical calculations are required to assess the roles of nearby oxygens and puckering of the nicotinamide ring on hydride transfer.

Other Cavities in ADH. Substitutions of other amino acid residues that interact with the coenzyme created cavities that were filled with a water or expelled a water. Val-292 was proposed to participate in PPV; its side chain is close to the nicotinamide ring, while its carbonyl oxygen interacts with N7N of the carboxamido group and C2N of the nicotinamide ring. Substitution of Val-292 (with Ala, Ser, or Thr) significantly increases (30−75-fold) the dissociation constants for the coenzymes, while the hydride transfer rate constants and catalytic efficiencies for benzyl alcohol oxidation decrease by 3−5-fold.[25,37] For V292S ADH, the logarithm of the rate constant for hydride transfer for benzyl alcohol oxidation is linearly dependent on the inverse temperature ($\Delta H^{\ddagger} \approx 13$ kcal/mol), whereas the logarithm of catalytic efficiency for benzaldehyde reduction exhibits a convex dependence on the inverse temperature that was fit by the van't Hoff equation ($\Delta H^{\ddagger} = 3.2$ kcal/mol, and $\Delta C_p^{\ddagger} \approx 250$ cal mol^{-1} K^{-1}). The isotope effects for the forward and reverse reactions catalyzed by the V292S enzyme are temperature-independent, providing evidence of vibrationally assisted, quantum mechanical tunneling in this enzyme.[25] We suggested that the convex van't Hoff dependence is evidence of protein fluctuations that affect the organization of reactants, as was also suggested for a thermophilic ADH.[82]

A structure of the V292S enzyme crystallized with NAD$^+$ and PFB determined at 2.0 Å resolution (PDB entry 1JU9) shows that the protein conformation is "open", similar to the

apoenzyme crystallized without added coenzyme (PDB entry 8ADH or 1YE3), and electron density for the nicotinamide ribose and PFB is lacking, indicating that the V292S substitution perturbs the conformational change that accompanies coenzyme and substrate binding. A new water molecule is observed in the cavity created by removal of a methyl group of Val-292. The V292S substitution appears to alter the equilibrium position for the conformational change of the enzyme–NAD$^+$ complex by a factor of 50, so that only 20% of the complex is in a state that would react with benzyl alcohol, as estimated from the 5-fold decrease in the catalytic efficiency, $V_1/(E_tK_b)$.[16] The substitution probably does not prevent the conformational change, as the structure of the V292T enzyme complexed with NAD$^+$ and pyrazole is in the closed conformation (PDB entry 1N8K).[37] The new water molecule is present in the closed conformation but is not in contact with the nicotinamide ring. The V292S enzyme apparently retains vibrationally assisted tunneling, and thus, the results do not provide evidence that supports, but also do not exclude, a role for Val-292 in PPV.

The double substitution, G293A/P295T, in a flexible loop of the coenzyme binding domain greatly (100−700-fold) increases steady-state kinetic constants and decreases the rate constant for benzyl alcohol oxidation to 1.3 s^{-1}, making hydride transfer rate-limiting for catalytic turnover.[83] A structure of the enzyme crystallized with NAD and TFE is in the open conformation, apparently unable to form the closed conformation because of steric clashes involving Ala-293 and Thr-295 (PDB entry 1QLH). A new (as compared to the apoenzyme, PDB entry 1YE3) water molecule is accommodated in the cavity because of the P295T substitution, with a hydrogen bond to Thr-295 OG1, and a second water is found in a cleft near Ala-293 O. Perhaps these waters help to stabilize the open conformation, but it is signficant that the enzyme retains high activity for hydride transfer.

In wild-type ADH, a water fills a cavity near the nicotinamide ring and makes hydrogen bonds with the carbonyl oxygen of Ala-317, the hydroxyl group of Ser-182 and the backbone N of Gly-320.[18,68] The carbonyl oxygen of Ala-317 also forms a hydrogen bond with N7N of the nicotinamide moiety. Ala-317 is replaced by a cysteine residue in human ADH4, and this was proposed to be the reason for the relatively large kinetic constants (10−100-fold larger) for ADH4 compared to those for horse ADH-E or human class I ADHs. However, the A317C substitution in horse ADH-E has very small effects on steady-state kinetic constants, even though the rate of hydride transfer from benzyl alcohol decreases by 2.8-fold.[84] The three-dimensional structure determined at 1.2 Å of the complex with NAD and PFB is almost identical with the structure of the wild-type enzyme, but the sulfhydryl group of Cys-317 displaces the water. It appears that the protein scaffold is relatively stable and can accommodate a water in a new cavity or the loss of water when a cavity is filled by substitution of an amino acid residue.

Perspectives on Catalysis by ADHs. It is generally believed that hydrogen is transferred with quantum mechanical tunneling in ADHs and that protein dynamics are involved. Geometries of substrates or substrate analogues in the complexes studied here approximate expected ground-state structures that could undergo direct hydrogen transfer after small reorganization that yields a tunneling-ready state with a calculated DAD of 3.2 Å[21,85] or closer to 2.7 Å for a calculated transition state.[86] The structures show that the geometries of

the active sites of V203A ADH complexes, in particular the complex with NAD and PFB, are very similar to those for wild-type ADH and raise a serious question about the proposal that an increased ground-state DAD for hydrogen transfer has led to diminished hydrogen tunneling for the V203A enzyme.[6,10,36] Why is hydrogen tunneling diminished in the V203A or F93W/V203A enzyme compared to that in the reference enzyme (F93W variant) if the ligands in both complexes are similarly preorganized and the ground-state DADs are similar? In terms of the rate equation based on the Marcus-like model currently proposed for hydrogen transfer, the simple explanation is that the energetic barrier $[E(r_x)]$ for the fluctuation of the DAD is altered.[68] Quantum mechanical tunneling may be particularly sensitive to the local motions and active site environment (including electrostatics[87]), and rates of catalysis may be compromised by small changes in protein structures. Perhaps the dynamics are altered because of increased flexibility (or puckering) in the positioning of the nicotinamide ring or the insertion of a water near the nicotinamide ring.[20,86] Nevertheless, investigations are required to explain quantitatively the results with the V207A and V203A enzymes, as discussed in recent reviews.[68,88,89]

An alternative explanation could be that tunneling is not actually diminished in the V203A enzyme but rather that kinetic complexity masks the tunneling, as was suggested for wild-type ADH.[22,24] This possibility seems unlikely, however, because the primary H/D isotope effect for catalytic turnover $[^DV_1/E_t$ (Table 2)] of 3.4 for V203A ADH indicates that hydride transfer is a major rate-limiting step in catalysis. (Because the temperature dependence of the isotope effects has not been determined for V203A ADH, evidence of thermally activated fluctuations of the DAD is not available.[68,85,90]) Although tunneling may be diminished in the V203A enzyme, quantum mechanical tunneling most likely still occurs, as that is an inherent characteristic of hydrogen transfer and because there are no apparent structural impediments for attaining a tunneling-ready state in the enzyme.

A related question is why the apparent rate of transfer of hydrogen from benzyl alcohol was decreased by the V203A substitution only from 24 to 1.5 s^{-1}, retaining perhaps most of the catalytic rate enhancement due to the enzyme,[59] if tunneling is diminished by a loss of PPV. The contribution of tunneling to the overall catalytic rate enhancement may be 2−20-fold.[3,42,91] The enormous remaining catalytic activity may be attributed to an appropriate active site scaffold, local environment, and thermal motions that conspire to produce a reactive state poised for hydride transfer.[19] Our estimates of mean fluctuations for protein and substrates from analysis of the B factors for both wild-type and V203A enzymes ranged up to ∼0.5 Å at 300 K. Such fluctuations suggest that DADs in substrates could approach the 2.7 Å distance for optimal hydride transfer, although substrates must also be oriented properly.

In this regard, it is interesting that mixed quantum mechanical/molecular dynamics calculations showed that substrate and protein interaction distances changed by ∼0.6 Å as the reactants proceeded toward the transition state along the reaction coordinate.[86] Curiously, when the DAD between NAD and alcohol decreased by 0.6 Å to 2.7 Å, the distance between C4N of NAD and the CG1 methyl group (labeled CG2 in the current structures) of Val-203 increased by 0.6 Å to 5.1 Å, as if the nicotinamide ring loses contact with Val-203. (The V203A substitution eliminates both methyl groups and

thus the contact with C4N, and the distance between C4N and 203 CA in all of the structures is ~5.4 Å.) Motions of other protein atoms were not illustrated, but the simulations showed that some contacts of the Val-203 side chain in wild-type enzyme are maintained: Val-203 CG2 to NAD C6N or Val-203 CG1 to Thr-178 CG1. Some interactions of the nicotinamide ring and the protein in the structures of wild-type and V203A enzymes are maintained: the side chain of Thr-178 with C4N, CG1 of Leu-292 with C2N, and the hydrogen bonds of the carboxamido group to the backbone atoms of residues 292, 317, and 319. Thus, the nicotinamide ring seems to have more restricted motions than the alcohol does, in accordance with the local *B* factors. The similarity of *B* factors of the ligands and residues 203 and 207 among these structures suggests that local dynamics are not altered much by the valine to alanine substitutions.

Understanding enzyme catalysis continues to provide fundamental challenges.[92] It appears that further experimental data and calculations are required to understand the links between protein dynamics and catalysis and to determine if nonequilibrium dynamics contribute.[80,81] A recent theoretical study of lactate dehydrogenase concluded that the V136A substitution at the nicotinamide binding site would result in dramatic changes in catalysis due to effects on PPV,[89] but most studies of temperature-dependent isotope effects focus on equilibrium motions and differences in DADs.[68,93,94] Perhaps PPV contribute to the hydrogen tunneling in optimally evolved wild-type enzymes,[90,95] but the protein scaffold, electrostatics, and local equilibrium motions may explain most of the enzyme catalysis.[96]

X-ray crystallography can determine some of the structures of the ensemble in the protein and within the active site and provide a framework for understanding the roles of dynamics in catalysis. Molecular dynamics simulations may provide information about the population of reactive complexes for complexes of mutated enzymes when starting structures are available,[19,97,90] but quantum mechanical calculations are required to correlate rate constants for hydride transfer with structures.[12] For future computations of the V203A enzyme, the starting model could be based on the F93W/V203A enzyme (PDB entry 1AXE, 2.0 Å) after the TFE is replaced with benzyl alcohol, if alternative conformations of amino acid side chains are not of interest. If the multitude of conformers, including ~50 amino acid residues with alternative conformations identified in the dimeric molecule, are of interest, the wild-type enzyme (PDB entry 4DWV, 1.14 Å) could be used after Val-203 is mutated *in silico* to alanine, waters A and B 994 are added in the positions found in the structures of the V203A enzyme, and fluorines are removed from the PFB.

A general challenge is to compute the rate constants for hydride transfer for a range of enzyme variants of ADH and show a correlation with experimental data. This may be difficult because many of the site-directed substitutions change the rate constant for hydride transfer by less than an order of magnitude. Even substitutions (e.g., V292S and G293A/P295T) that greatly increase steady-state kinetic constants, decrease the overall catalytic efficiency $[V_1/(E_tK_bK_{ia})$ for alcohol oxidation], and alter the energetics of the conformational change have modest effects on the rate constant for hydride transfer.[16,59] Anticorrelated motions of the catalytic and coenzyme binding domains that are related to the relatively slow global conformational change that accompanies coenzyme binding are suggested to "push" the substrates in the Michaelis complex toward a reactive state,[40,41,98] but the contribution to hydride transfer may be modest. Substitutions of amino acid residues distant from the nicotinamide binding site also have modest effects on turnover and catalytic efficiency.[23,29,99] Local structures and catalysis can be altered by substitutions of amino acid residues, but the protein scaffold can maintain the constellation of the many residues participating in catalysis. These considerations lead us to suggest that once the substrates are bound, local motions are more important than global motions for the chemistry of hydrogen transfer.

■ ASSOCIATED CONTENT

Accession Codes

The X-ray coordinates and structure factors have been deposited in the Protein Data Bank as entries 4NG5 for the V203A enzyme complexed with NAD⁺ and 2,3,4,5,6-penta-fluorobenzyl alcohol, 4NFS for the V203A enzyme complexed with NAD⁺ and 2,2,2-trifluoroethanol, and 4NFH for the V207A enzyme complexed with NAD⁺ and 2,3,4,5,6-penta-fluorobenzyl alcohol.

■ AUTHOR INFORMATION

Corresponding Author

*E-mail: bv-plapp@uiowa.edu. Phone: (319) 335-7909. Fax: (319) 335-9570.

Present Addresses

†A.Y.: Department of Microbiology, The University of Iowa, Iowa City, IA 52242-1109.
‡J.K.R.: Kemin Industries, 2100 Maury St., Des Moines, IA 50306.

Notes

The authors declare no competing financial interests.

■ ABBREVIATIONS

ADH, alcohol dehydrogenase; V203A, amino acid substitution in which Val-203 was substituted with Ala-203; WT, wild-type; PFB, 2,3,4,5,6-pentafluorobenzyl alcohol; TFE, 2,2,2-trifluoroethanol; rmsd, root-mean-square deviation; PPV, protein-promoting vibrations; DAD, donor−acceptor distance.

■ REFERENCES

(1) Cha, Y., Murray, C. J., and Klinman, J. P. (1989) Hydrogen tunneling in enzyme reactions. *Science 243*, 1325−1330.

(2) Basran, J., Sutcliffe, M. J., and Scrutton, N. S. (1999) Enzymatic H-transfer requires vibration-driven extreme tunneling. *Biochemistry 38*, 3218−3222.

(3) Billeter, S. R., Webb, S. P., Iordanov, T., Agarwal, P. K., and Hammes-Schiffer, S. (2001) Hybrid approach for including electronic and nuclear quantum effects in molecular dynamics simulations of hydrogen transfer reactions in enzymes. *J. Chem. Phys. 114*, 6925−6936.

(4) Antoniou, D., Caratzoulas, S., Kalyanaraman, C., Mincer, J. S., and Schwartz, S. D. (2002) Barrier passage and protein dynamics in enzymatically catalyzed reactions. *Eur. J. Biochem. 269*, 3103−3112.

(5) Knapp, M. J., and Klinman, J. P. (2002) Environmentally coupled hydrogen tunneling: Linking catalysis to dynamics. *Eur. J. Biochem. 269*, 3113−3121.

(6) Klinman, J. P. (2009) An integrated model for enzyme catalysis emerges from studies of hydrogen tunneling. *Chem. Phys. Lett. 471*, 179−193.

(7) Hammes-Schiffer, S. (2002) Impact of enzyme motion on activity. *Biochemistry 41*, 13335−13343.

(8) Sutcliffe, M. J., and Scrutton, N. S. (2002) A new conceptual framework for enzyme catalysis. Hydrogen tunnelling coupled to enzyme dynamics in flavoprotein and quinoprotein enzymes. *Eur. J. Biochem. 269*, 3096−3102.

(9) Hay, S., Johannissen, L. O., Sutcliffe, M. J., and Scrutton, N. S. (2010) Barrier compression and its contribution to both classical and quantum mechanical aspects of enzyme catalysis. *Biophys. J. 98*, 121−128.

(10) Nagel, Z. D., and Klinman, J. P. (2010) Update 1 of: Tunneling and dynamics in enzymatic hydride transfer. *Chem. Rev. 110*, PR41−PR67.

(11) Agarwal, P. K., Billeter, S. R., Rajagopalan, P. T. R., Benkovic, S. J., and Hammes-Schiffer, S. (2002) Network of coupled promoting motions in enzyme catalysis. *Proc. Natl. Acad. Sci. U.S.A. 99*, 2794−2799.

(12) Hammes-Schiffer, S. (2013) Catalytic efficiency of enzymes: A theoretical analysis. *Biochemistry 52*, 2012−2020.

(13) Nagel, Z. D., Cun, S., and Klinman, J. P. (2013) Identification of a long-range protein network that modulates active site dynamics in extremophilic alcohol dehydrogenases. *J. Biol. Chem. 288*, 14087−14097.

(14) Eklund, H., Samama, J. P., Wallén, L., Brändén, C. I., Åkeson, Å., and Jones, T. A. (1981) Structure of a triclinic ternary complex of horse liver alcohol dehydrogenase at 2.9 Å resolution. *J. Mol. Biol. 146*, 561−587.

(15) Eklund, H., and Ramaswamy, S. (2008) Medium- and short-chain dehydrogenase/reductase gene and protein families: Three-dimensional structures of MDR alcohol dehydrogenases. *Cell. Mol. Life Sci. 65*, 3907−3917.

(16) Plapp, B. V. (2010) Conformational changes and catalysis by alcohol dehydrogenase. *Arch. Biochem. Biophys. 493*, 3−12.

(17) Venkataramaiah, T. H., and Plapp, B. V. (2003) Formamides mimic aldehydes and inhibit liver alcohol dehydrogenases and ethanol metabolism. *J. Biol. Chem. 278*, 36699−36706.

(18) Plapp, B. V., and Ramaswamy, S. (2012) Atomic-resolution structures of horse liver alcohol dehydrogenase with NAD$^+$ and fluoroalcohols define strained Michaelis complexes. *Biochemistry 51*, 4035−4048.

(19) Luo, J., and Bruice, T. C. (2001) Dynamic structures of horse liver alcohol dehydrogenase (HLADH): Results of molecular dynamics simulations of HLADH-NAD$^+$-PhCH$_2$OH, HLADH-NAD$^+$-PhCH$_2$O$^-$, and HLADH-NADH-PhCHO. *J. Am. Chem. Soc. 123*, 11952−11959.

(20) Webb, S. P., Agarwal, P. K., and Hammes-Schiffer, S. (2000) Combining electronic structure methods with the calculation of hydrogen vibrational wavefunctions: Application to hydride transfer in liver alcohol dehydrogenase. *J. Phys. Chem. B 104*, 8884−8894.

(21) Roston, D., and Kohen, A. (2010) Elusive transition state of alcohol dehydrogenase unveiled. *Proc. Natl. Acad. Sci. U.S.A. 107*, 9572−9577.

(22) Bahnson, B. J., Park, D. H., Kim, K., Plapp, B. V., and Klinman, J. P. (1993) Unmasking of hydrogen tunneling in the horse liver alcohol dehydrogenase reaction by site-directed mutagenesis. *Biochemistry 32*, 5503−5507.

(23) Chin, J. K., and Klinman, J. P. (2000) Probes of a role for remote binding interactions on hydrogen tunneling in the horse liver alcohol dehydrogenase reaction. *Biochemistry 39*, 1278−1284.

(24) Tsai, S., and Klinman, J. P. (2001) Probes of hydrogen tunneling with horse liver alcohol dehydrogenase at subzero temperatures. *Biochemistry 40*, 2303−2311.

(25) Rubach, J. K., Ramaswamy, S., and Plapp, B. V. (2001) Contributions of valine-292 in the nicotinamide binding site of liver alcohol dehydrogenase and dynamics to catalysis. *Biochemistry 40*, 12686−12694.

(26) Caratzoulas, S., Mincer, J. S., and Schwartz, S. D. (2002) Identification of a protein-promoting vibration in the reaction catalyzed by horse liver alcohol dehydrogenase. *J. Am. Chem. Soc. 124*, 3270−3276.

(27) Antoniou, D., Basner, J., Núñez, S., and Schwartz, S. D. (2006) Computational and theoretical methods to explore the relation between enzyme dynamics and catalysis. *Chem. Rev. 106*, 3170−3187.

(28) Schwartz, S. D. (2006) Vibrationally enhanced tunneling and kinetic isotope effects in enzymatic reaction. In *Isotope Effects in Chemistry and Biology* (Kohen, A., and Limbach, H. H., Eds.) pp 475−498, Taylor & Francis, CRC Press, Boca Raton, FL.

(29) Fan, F., and Plapp, B. V. (1995) Substitutions of isoleucine residues at the adenine binding site activate horse liver alcohol dehydrogenase. *Biochemistry 34*, 4709−4713.

(30) Sun, H. W., and Plapp, B. V. (1992) Progressive sequence alignment and molecular evolution of the Zn-containing alcohol dehydrogenase family. *J. Mol. Evol. 34*, 522−535.

(31) Buckle, A. M., Cramer, P., and Fersht, A. R. (1996) Structural and energetic responses to cavity-creating mutations in hydrophobic cores: Observation of a buried water molecule and the hydrophilic nature of such hydrophobic cavities. *Biochemistry 35*, 4298−4305.

(32) Matthews, B. W., and Liu, L. (2009) A review about nothing: Are apolar cavities in proteins really empty? *Protein Sci. 18*, 494−502.

(33) Baase, W. A., Liu, L., Tronrud, D. E., and Matthews, B. W. (2010) Lessons from the lysozyme of phage T4. *Protein Sci. 19*, 631−641.

(34) Xu, J. A., Baase, W. A., Baldwin, E., and Matthews, B. W. (1998) The response of T4 lysozyme to large-to-small substitutions within the core and its relation to the hydrophobic effect. *Protein Sci. 7*, 158−177.

(35) Bueno, M., Campos, L. A., Estrada, J., and Sancho, J. (2006) Energetics of aliphatic deletions in protein cores. *Protein Sci. 15*, 1858−1872.

(36) Bahnson, B. J., Colby, T. D., Chin, J. K., Goldstein, B. M., and Klinman, J. P. (1997) A link between protein structure and enzyme catalyzed hydrogen tunneling. *Proc. Natl. Acad. Sci. U.S.A. 94*, 12797−12802.

(37) Rubach, J. K., and Plapp, B. V. (2003) Amino acid residues in the nicotinamide binding site contribute to catalysis by horse liver alcohol dehydrogenase. *Biochemistry 42*, 2907−2915.

(38) Colby, T. D., Bahnson, B. J., Chin, J. K., Klinman, J. P., and Goldstein, B. M. (1998) Active site modifications in a double mutant of liver alcohol dehydrogenase: Structural studies of two enzyme-ligand complexes. *Biochemistry 37*, 9295−9304.

(39) Luo, J., Kahn, K., and Bruice, T. C. (1999) The linear dependence of log(k_{cat}/K_m) for reduction of NAD$^+$ by PhCH$_2$OH on the distance between reactants when catalyzed by horse liver alcohol dehydrogenase and 203 single point mutants. *Bioorg. Chem. 27*, 289–296.

(40) Luo, J., and Bruice, T. C. (2004) Anticorrelated motions as a driving force in enzyme catalysis: The dehydrogenase reaction. *Proc. Natl. Acad. Sci. U.S.A. 101*, 13152–13156.

(41) Luo, J., and Bruice, T. C. (2007) Low-frequency normal modes in horse liver alcohol dehydrogenase and motions of residues involved in the enzymatic reaction. *Biophys. Chem. 126*, 80–85.

(42) Cui, Q., and Karplus, M. (2002) Promoting modes and demoting modes in enzyme-catalyzed proton transfer reactions: A study of models and realistic systems. *J. Phys. Chem. B 106*, 7927–7947.

(43) Nagel, Z. D., Meadows, C. W., Dong, M., Bahnson, B. J., and Klinman, J. P. (2012) Active site hydrophobic residues impact hydrogen tunneling differently in a thermophilic alcohol dehydrogenase at optimal versus nonoptimal temperatures. *Biochemistry 51*, 4147–4156.

(44) Ganzhorn, A. J., and Plapp, B. V. (1988) Carboxyl groups near the active site zinc contribute to catalysis in yeast alcohol dehydrogenase. *J. Biol. Chem. 263*, 5446–5454.

(45) Park, D.-H., and Plapp, B. V. (1991) Isoenzymes of horse liver alcohol dehydrogenase active on ethanol and steroids. cDNA cloning, expression, and comparison of active sites. *J. Biol. Chem. 266*, 13296–13302.

(46) Plapp, B. V. (1970) Enhancement of the activity of horse liver alcohol dehydrogenase by modification of amino groups at the active sites. *J. Biol. Chem. 245*, 1727–1735.

(47) Theorell, H., and Yonetani, T. (1963) Liver alcohol dehydrogenase-DPN-pyrazole complex: A model of a ternary intermediate in the enzyme reaction. *Biochem. Z. 338*, 537–553.

(48) Cleland, W. W. (1979) Statistical analysis of enzyme kinetic data. *Methods Enzymol. 63*, 103–138.

(49) Kabsch, W. (2010) XDS. *Acta Crystallogr. D66*, 125–132.

(50) Pflugrath, J. W. (1999) The finer things in X-ray diffraction data collection. *Acta Crystallogr. D55*, 1718–1725.

(51) Winn, M. D., Ballard, C. C., Cowtan, K. D., Dodson, E. J., Emsley, P., Evans, P. R., Keegan, R. M., Krissinel, E. B., Leslie, A. G., McCoy, A., McNicholas, S. J., Murshudov, G. N., Pannu, N. S., Potterton, E. A., Powell, H. R., Read, R. J., Vagin, A., and Wilson, K. S. (2011) Overview of the CCP4 suite and current developments. *Acta Crystallogr. D67*, 235–242.

(52) Jones, T. A., Zou, J. Y., Cowan, S. W., and Kjeldgaard, M. (1991) Improved methods for building protein models in electron density maps and the location of errors in these models. *Acta Crystallogr. A47* (Part 2), 110–119.

(53) Kleywegt, G. J., and Jones, T. A. (1994) Detection, delineation, measurement and display of cavities in macromolecular structures. *Acta Crystallogr. D50*, 178–185.

(54) Harris, M., and Jones, T. A. (2001) Molray: A web interface between O and the POV-Ray ray tracer. *Acta Crystallogr. D57*, 1201–1203.

(55) Sheldrick, G. M. (2008) A short history of SHELX. *Acta Crystallogr. A64*, 112–122.

(56) Park, D.-H., and Plapp, B. V. (1992) Interconversion of E and S isoenzymes of horse liver alcohol dehydrogenase. Several residues contribute indirectly to catalysis. *J. Biol. Chem. 267*, 5527–5533.

(57) Dworschack, R. T., and Plapp, B. V. (1977) Kinetics of native and activated isozymes of horse liver alcohol dehydrogenase. *Biochemistry 16*, 111–116.

(58) Dalziel, K. (1963) Kinetic studies of liver alcohol dehydrogenase and pH effects with coenzyme preparations of high purity. *J. Biol. Chem. 238*, 2850–2858.

(59) Plapp, B. V. (2006) Catalysis by alcohol dehydrogenases. In *Isotope Effects in Chemistry and Biology* (Kohen, A., and Limbach, H. H., Eds.) pp 811–835, Taylor & Francis, CRC Press, Boca Raton, FL.

(60) Sekhar, V. C., and Plapp, B. V. (1990) Rate constants for a mechanism including intermediates in the interconversion of ternary complexes by horse liver alcohol dehydrogenase. *Biochemistry 29*, 4289–4295.

(61) Gibbons, B. J., and Hurley, T. D. (2004) Structure of three class I human alcohol dehydrogenases complexed with isoenzyme specfic formamide inhibitors. *Biochemistry 43*, 12555–12562.

(62) Dietrich, H., MacGibbon, A. K., Dunn, M. F., and Zeppezauer, M. (1983) Investigation of the pH dependencies of coenzyme binding to liver alcohol dehydrogenase lacking zinc ion at the active sites. *Biochemistry 22*, 3432–3438.

(63) Schneider, G., Eklund, H., Cedergren-Zeppezauer, E., and Zeppezauer, M. (1983) Structure of the complex of active site metal-depleted horse liver alcohol dehydrogenase and NADH. *EMBO J. 2*, 685–689.

(64) Schneider, G., Eklund, H., Cedergren Zeppezauer, E., and Zeppezauer, M. (1983) Crystal structures of the active site in specifically metal-depleted and cobalt-substituted horse liver alcohol dehydrogenase derivatives. *Proc. Natl. Acad. Sci. U.S.A. 80*, 5289–5293.

(65) Cho, H., Ramaswamy, S., and Plapp, B. V. (1997) Flexibility of liver alcohol dehydrogenase in stereoselective binding of 3-butylthiolane 1-oxides. *Biochemistry 36*, 382–389.

(66) Meijers, R., and Cedergren-Zeppezauer, E. (2009) A variety of electrostatic interactions and adducts can activate NAD(P) cofactors for hydride transfer. *Chem.-Biol. Interact. 178*, 24–28.

(67) Hammes, G. G., Benkovic, S. J., and Hammes-Schiffer, S. (2011) Flexibility, diversity, and cooperativity: Pillars of enzyme catalysis. *Biochemistry 50*, 10422–10430.

(68) Klinman, J. P., and Kohen, A. (2013) Hydrogen tunneling links protein dynamics to enzyme catalysis. *Annu. Rev. Biochem. 82*, 471–496.

(69) Merritt, E. A. (1999) Comparing anisotropic displacement parameters in protein structures. *Acta Crystallogr. D55*, 1997–2004.

(70) Wilson, M. A., and Brunger, A. T. (2000) The 1.0 Å crystal structure of Ca^{2+}-bound calmodulin: An analysis of disorder and implications for functionally relevant plasticity. *J. Mol. Biol. 301*, 1237–1256.

(71) Winn, M. D., Isupov, M. N., and Murshudov, G. N. (2001) Use of TLS parameters to model anisotropic displacements in macro-molecular refinement. *Acta Crystallogr. D57*, 122–133.

(72) Painter, J., and Merritt, E. A. (2006) Optimal description of a protein structure in terms of multiple groups undergoing TLS motion. *Acta Crystallogr. D62*, 439–450.

(73) Schmidt, A., and Lamzin, V. S. (2010) Internal motion in protein crystal structures. *Protein Sci. 19*, 944–953.

(74) Winn, M. D., Murshudov, G. N., and Papiz, M. Z. (2003) Macromolecular TLS refinement in REFMAC at moderate resolutions. *Methods Enzymol. 374*, 300–321.

(75) Tilton, R. F., Jr., Dewan, J. C., and Petsko, G. A. (1992) Effects of temperature on protein structure and dynamics: X-ray crystallographic studies of the protein ribonuclease-A at nine different temperatures from 98 to 320 K. *Biochemistry 31*, 2469–2481.

(76) Chong, S. H., Joti, Y., Kidera, A., Go, N., Ostermann, A., Gassmann, A., and Parak, F. (2001) Dynamical transition of myoglobin in a crystal: Comparative studies of X-ray crystallography and Mossbauer spectroscopy. *Eur. Biophys. J. 30*, 319–329.

(77) Petrova, T., Ginell, S., Mitschler, A., Hazemann, I., Schneider, T., Cousido, A., Lunin, V. Y., Joachimiak, A., and Podjarny, A. (2006) Ultrahigh-resolution study of protein atomic displacement parameters at cryotemperatures obtained with a helium cryostat. *Acta Crystallogr. D62*, 1535–1544.

(78) Joti, Y., Nakasako, M., Kidera, A., and Go, N. (2002) Nonlinear temperature dependence of the crystal structure of lysozyme: Correlation between coordinate shifts and thermal factors. *Acta Crystallogr. D58*, 1421–1432.

(79) Cui, Q., Elstner, M., and Karplus, M. (2002) A theoretical analysis of the proton and hydride transfer in liver alcohol dehydrogenase (LADH). *J. Phys. Chem. B 106*, 2721–2740.

(80) Schwartz, S. D. (2013) Protein dynamics and the enzymatic reaction coordinate. *Top. Curr. Chem. 337*, 189−208.

(81) Antoniou, D., and Schwartz, S. D. (2011) Protein dynamics and enzymatic chemical barrier passage. *J. Phys. Chem. B 115*, 15147−15158.

(82) Kohen, A., Cannio, R., Bartolucci, S., and Klinman, J. P. (1999) Enzyme dynamics and hydrogen tunnelling in a thermophilic alcohol dehydrogenase. *Nature 399*, 496−499.

(83) Ramaswamy, S., Park, D.-H., and Plapp, B. V. (1999) Substitutions in a flexible loop of horse liver alcohol dehydrogenase hinder the conformational change and unmask hydrogen transfer. *Biochemistry 38*, 13951−13959.

(84) Herdendorf, T. J., and Plapp, B. V. (2011) Origins of the high catalytic activity of human alcohol dehydrogenase 4 studied with horse liver A317C alcohol dehydrogenase. *Chem.-Biol. Interact. 191*, 42−47.

(85) Roston, D., Cheatum, C. M., and Kohen, A. (2012) Hydrogen donor-acceptor fluctuations from kinetic isotope effects: A phenomenological model. *Biochemistry 51*, 6860−6870.

(86) Billeter, S. R., Webb, S. P., Agarwal, P. K., Iordanov, T., and Hammes-Schiffer, S. (2001) Hydride transfer in liver alcohol dehydrogenase: Quantum dynamics, kinetic isotope effects, and role of enzyme motion. *J. Am. Chem. Soc. 123*, 11262−11272.

(87) Warshel, A. (1998) Electrostatic origin of the catalytic power of enzymes and the role of preorganized active sites. *J. Biol. Chem. 273*, 27035−27038.

(88) Roston, D., Islam, Z., and Kohen, A. (2013) Isotope effects as probes for enzyme catalyzed hydrogen-transfer reactions. *Molecules 18*, 5543−5567.

(89) Masterson, J. E., and Schwartz, S. D. (2013) Changes in protein architecture and subpicosecond protein dynamics impact the reaction catalyzed by lactate dehydrogenase. *J. Phys. Chem. A 117*, 7107−7113.

(90) Stojković, V., Perissinotti, L. L., Willmer, D., Benkovic, S. J., and Kohen, A. (2012) Effects of the donor−acceptor distance and dynamics on hydride tunneling in the dihydrofolate reductase catalyzed reaction. *J. Am. Chem. Soc. 134*, 1738−1745.

(91) Gao, J., and Truhlar, D. G. (2002) Quantum mechanical methods for enzyme kinetics. *Annu. Rev. Phys. Chem. 53*, 467−505.

(92) Herschlag, D., and Natarajan, A. (2013) Fundamental challenges in mechanistic enzymology: Progress toward understanding the rate enhancements of enzymes. *Biochemistry 52*, 2050−2067.

(93) Klinman, J. P. (2013) Importance of protein dynamics during enzymatic C−H bond cleavage catalysis. *Biochemistry 52*, 2068−2077.

(94) Cheatum, C. M., and Kohen, A. (2013) Relationship of femtosecond-picosecond dynamics to enzyme-catalyzed H-transfer. *Top. Curr. Chem. 337*, 1−39.

(95) Yahashiri, A., Howell, E. E., and Kohen, A. (2008) Tuning of the H-transfer coordinate in primitive versus well-evolved enzymes. *ChemPhysChem 9*, 980−982.

(96) Villà, J., and Warshel, A. (2001) Energetics and dynamics of enzymatic reactions. *J. Phys. Chem. B 105*, 7887−7907.

(97) Luo, J., and Bruice, T. C. (2002) Ten-nanosecond molecular dynamics simulation of the motions of the horse liver alcohol dehydrogenase·PhCH$_2$O$^-$ complex. *Proc. Natl. Acad. Sci. U.S.A. 99*, 16597−16600.

(98) Bruice, T. C. (2006) Computational approaches: Reaction trajectories, structures, and atomic motions. Enzyme reactions and proficiency. *Chem. Rev. 106*, 3119−3139.

(99) Strasser, F., Dey, J., Eftink, M. R., and Plapp, B. V. (1998) Activation of horse liver alcohol dehydrogenase upon substitution of tryptophan 314 at the dimer interface. *Arch. Biochem. Biophys. 358*, 369−376.

(100) Klinman, J. P. (1972) The mechanism of enzyme-catalyzed reduced nicotinamide adenine dinucleotide-dependent reductions. Substituent and isotope effects in the yeast alcohol dehydrogenase reaction. *J. Biol. Chem. 247*, 7977−7987.

(101) Weidig, C. F., Halvorson, H. R., and Shore, J. D. (1977) Evidence for site equivalence in the reaction mechanism of horse liver alcohol dehydrogenase with aromatic substrates at alkaline pH. *Biochemistry 16*, 2916−2922.

(102) Dunn, M. F., Bernhard, S. A., Anderson, D., Copeland, A., Morris, R. G., and Roque, J. P. (1979) On site-site interactions in the liver alcohol dehydrogenase catalytic mechanism. *Biochemistry 18*, 2346−2354.

(103) Brunger, A. T. (1992) Free R-value: A novel statistical quantity for assessing the accuracy of crystal structures. *Nature 355*, 472−475.

(104) Merritt, E. A. (1999) Expanding the model: Anisotropic displacement parameters in protein structure refinement. *Acta Crystallogr. D55*, 1109−1117.

(105) Meijers, R., Morris, R. J., Adolph, H. W., Merli, A., Lamzin, V. S., and Cedergren-Zeppezauer, E. S. (2001) On the enzymatic activation of NADH. *J. Biol. Chem. 276*, 9316−9321.